Antiviral Research 154 (2018) 116–123

Contents lists available at ScienceDirect

Antiviral Research

journal homepage: www.elsevier.com/locate/antiviral

Inhibition of dengue virus infection by mannoside glycolipid conjugates

Evelyne Schaeffer[a], Vincent Flacher[a], Patrick Neuberg[b], Astrid Hoste[a], Adrien Brulefert[a], Jean-Daniel Fauny[a], Alain Wagner[b], Christopher G. Mueller[a,*]

[a] CNRS, Université de Strasbourg, Immunopathology and Therapeutic Chemistry, UPR 3572, 67000 Strasbourg, France
[b] CNRS, Université de Strasbourg, Laboratory of Functional Chemo Systems, UMR 7199, 67400 Illkirch, France

ARTICLE INFO

Keywords:
Dengue virus
Dendritic cells
Macrophages
Skin
Inhibitors
Cell membrane

ABSTRACT

Dengue virus (DENV), a mosquito-borne flavivirus, causes severe and potentially fatal symptoms in millions of infected individuals each year. Although dengue fever represents a major global public health problem, the vaccines or antiviral drugs proposed so far have not shown sufficient efficacy and safety, calling for new antiviral developments. Here we have shown that a mannoside glycolipid conjugate (MGC) bearing a trimannose head with a saturated lipid chain inhibited DENV productive infection. It showed remarkable cell promiscuity, being active in human skin dendritic cells, hepatoma cell lines and Vero cells, and was active against all four DENV serotypes, with an IC_{50} in the low micromolar range. Time-of-addition experiments and structure-activity analyses revealed the importance of the lipid chain to interfere with an early viral infection step. This, together with a correlation between antiviral activity and membrane polarization by the lipid moiety indicated that the inhibitor functions by blocking viral envelope fusion with the endosome membrane. These finding establish MGCs as a novel class of antivirals against the DENV.

1. Introduction

Infection by Dengue virus (DENV) is a major cause of disease in tropical and subtropical areas, with at least 100 million clinical cases occurring each year, and more than 2.5 billion people at risk (Bhatt et al., 2013; Stanaway et al., 2016). DENV is an arthropod-borne single-stranded RNA virus of the *Flavivirus* genus, transmitted to humans by infected *Aedes* mosquitoes. It comprises four related but antigenically distinct serotypes, DENV-1, -2, -3, and -4. To restrict the burden on public health, studies have concentrated on the elaboration of vaccines, but the complex immunopathology of dengue has hampered their development and efficacy. No specific vaccine and no antiviral drug have been licensed for clinical use; for review see (Julander et al., 2011; Lo and Perng, 2016; Rather et al., 2017).

DENV cell-entry is mediated by a number of receptors (Kaufmann and Rossmann, 2011) including the C-type lectins Dendritic Cell-Specific Intercellular adhesion molecule-3-Grabbing Nonintegrin (DC-SIGN/CD209) (Navarro-Sanchez et al., 2003; Tassaneetrithep et al., 2003) and the mannose receptor (MR/CD206) (Miller et al., 2008) expressed by dendritic cells (DCs) and macrophages. Early in DENV infection the first events decisive for disease development are likely to occur in the skin. It has been shown that after virus inoculation by the mosquito, dermal DCs and macrophages are the primary targets of infection (Cerny et al., 2014; Duyen et al., 2017; Ivory et al., 2015; Schaeffer et al., 2015; Schmid et al., 2014).

In the search of DENV inhibitors, both viral and host proteins essential for the viral replication cycle have been tested as potential targets for antiviral development (see review, (Noble et al., 2010)). For example, some strategies target viral RNA replication (Diamond et al., 2002), the NS2B-NS3 protease (Chu et al., 2015), or the viral envelope protein (Jadav et al., 2015), while others target cellular enzymes that act as regulators of lipid homeostasis (Hyrina et al., 2017). The nucleoside analogue balapiravir blocks viral RNA synthesis by acting as a chain terminator. Chloroquine inhibits the fusion of the viral membrane with that of the endosome, as well as virus maturation. Lovastatin inhibits virus entry, maturation and egress. Celgosivir impairs proper glycosylation of the DENV E, prM and NS1 proteins. So far, no obvious beneficial clinical effect was detected with any of these compounds (Kaptein and Neyts, 2016). This emphasizes the need for continuous research to find new anti-DENV drugs.

Mannoside glycolipid conjugates (MGCs) are formed by three building blocks: a tri-mannose head, a hydrophilic linker and a hydrophobic lipid chain. They are water-soluble and can self-assemble into micelles. Our previous studies have shown that MGCs interact with

Abbreviations: DENV, dengue virus; DC, dendritic cell; MDDC, monocyte-derived dendritic cells; IC_{50}, 50% inhibitory concentration; IL-4, Interleukin-4; MGC, mannoside glycolipid conjugate

* Corresponding author. CNRS UPR 3572, Institut de Biologie Moléculaire et Cellulaire, 15 rue René Descartes, 67084 Strasbourg Cedex, France.
E-mail address: c.mueller@ibmc-cnrs.unistra.fr (C.G. Mueller).

https://doi.org/10.1016/j.antiviral.2018.04.005
Received 21 December 2017; Received in revised form 6 March 2018; Accepted 5 April 2018
Available online 06 April 2018
0166-3542/

lectin cell surface receptors that bind glycosylated molecules (Dehuyser et al., 2012; Schaeffer et al., 2013). Because DENV is glycosylated on the envelope protein, it appeared attractive to test the ability of MGCs to inhibit DENV infection. Interestingly, MGCs also antagonize Toll-like receptor type 4 signaling by lipopolysaccharide (LPS), although this receptor or its co-receptor CD14 do not bind MGCs (Flacher et al., 2015). This suggests that the biological properties of MGCs may not only be mediated by a specific interaction with lectin receptors.

In this report, we have tested whether MGCs display antiviral activity against DENV and have investigated the underlying mechanism. We find that a MGC, referred here as MGC 2, inhibits infection of primary human DCs, hepatoma and Vero cell lines. Using time-of-addition experiments, we show data supporting the conclusion that an early infection step is inhibited. Further, by visualization and quantitative image analysis we provide supporting evidence that a disruption of normal cell membrane composition may be the underlying mechanisms of blockage of viral life cycle initiation.

2. Material and methods

2.1. Viruses, virus titration and cells

The pDENV-2 replicon of DENV-2 (strain 16681) was generously provided by Dr. E. Harris (University of California, Berkeley, USA). The clinical isolates DENV-1 (CRBIP 10.1), DENV-2 (RO7/2259), DENV-3 (CRBIP 10.3), and DENV-4 (VIMFH4) were a generous gift of Dr Anavaj Sakuntabhai (Institut Pasteur, Paris, France). Viruses were produced in C6/36 *Aedes albopictus* mosquito cells, as described (Schaeffer et al., 2015). Titers in cell-free supernatants were determined by infection of Vero cells as described (Lambeth et al., 2005). Infectivity titers were expressed as FACS-infectious units (FIU)/ml.

African green monkey kidney Vero cells and human hepatoma HepG2 cells were cultured at 37 °C in Dulbecco's modified Eagle's medium (DMEM, Lonza) supplemented with 10% (v/v) heat-inactivated fetal bovine serum (FBS) and gentamycin. Human monocytic THP-1 and primary cells were cultured at 37 °C in RPMI 1640 supplemented with gentamycin and 10% (v/v) FBS (complete medium). Human monocytes were purified from buffy coats by successive Ficoll and Percoll gradients. Monocyte-derived dendritic cells (MDDCs) were differentiated from monocytes by 5 days of culture with GM-CSF (50 ng/ml, ImmunoTools) and IL-4 (10 ng/ml, ImmunoTools), as described. Abdominal skin was obtained with written informed consent and institutional review board approval, in agreement with the Helsinki Declaration and French legislation. Dermal dendritic cells (dDCs) and dermal macrophages were isolated from surgical explants of human skin, as previously described (Schaeffer et al., 2015). Briefly, dDCs were allowed to migrate out of the skin for 2 days into a medium lacking or containing IL-4. The non-migratory macrophages were isolated from the tissue by enzymatic digestion. After culturing the dermal cell suspension for 2 days, $CD14^+HLA\text{-}DR^+$ cells were purified by flow cytometric cell sorting (Schaeffer et al., 2015).

2.2. Compounds

Compounds MGC 2 and 2U were synthesized by the company Roowin (Riom, France). Other MGCs were synthesized at the Laboratory of Functional Chemo Systems (Illkirch, France). The syntheses, physico-chemical properties and cytotoxicities of MGCs were previously reported (Dehuyser et al., 2012; Flacher et al., 2015; Schaeffer et al., 2013). All compounds were dissolved in water.

2.3. Cell cytotoxicity assay

The effect of MGC 2 on cell viability was assessed by monitoring the reduction by cellular deshydrogenases of the tetrazolium salt WST-1 to dark yellow colored formazan, using the Cell Proliferation Reagent WST-1 (Roche). Human cells (10^5 MDDCs, 5×10^4 dDCs, 2×10^4 HepG2 cells) in 96-well culture plates were treated in quadruplicate with different concentrations of MGC 2, medium alone, or 1% Triton-X100 at 37 °C. After 24 h, WST-1 stock solution diluted 10-fold in cell culture medium (50 µL) was added at 37 °C. After 1 h (HepG2 cells) or 4 h (dDCs, MDDCs), the optical density of the resulting solutions was measured at 450 nm using a microplate reader (Multiskan FC, Thermo Scientific).

2.4. Antiviral assays

2.4.1. Inhibition assays

Assays were performed in 48-well plates. MDDCs (2×10^5 cells) and skin-purified cells (0.5×10^5 cells) were preincubated with compounds for 30 min before exposure to DENV-2 (MOI of respectively 0.2 and 0.5). In time-of-addition assays, cells were treated with MGC 2 according to the indicated timing. HepG2 cells (0.5×10^5 cells) were exposed to DENV-1, -2, -3, or -4 after 30 min of pre-treatment with MGC 2. After incubation for 2 h at 37 °C in serum-free medium, cells were washed and cultured in complete medium. After 2 days, cells infected with DENV-2 were labeled for intracellular viral envelope protein with mouse anti-dengue type 2 virus monoclonal antibody (clone 3H5.1, Millipore MAB8702) and stained with APC rat anti-mouse IgG1 (BD Biosciences). Cells infected with DENV-1, -2, -3, -4 were analyzed with mouse anti-dengue complex monoclonal antibody (clone D3-2H2-9, Millipore, MAB 8705) followed by APC rat anti-mouse IgG2a (BD Biosciences). Fluorescence was measured by flow cytometry (FACSCalibur, Becton Dickinson) and the data analyzed using Cell Quest Pro (BD Bioscience) or FlowJo (TreeStar).

2.4.2. Viral cell-entry by confocal microscopy

Cells were pre-treated in medium without serum with MGC 2 (100 µM) for 30 min or left untreated, exposed to DENV-2 for 1 h, and subjected or not to wash/chase by extensive washes and incubation in complete medium for 1 h, before fixation, permeabilization and labeling of DENV-E using Cy3-conjugated mAb 4G2 (kind gift from Philippe Desprès, Institut Pasteur, Paris, France). Cells were labeled with DiD (5 µg/ml, Thermo Fisher Scientific) for 10 min at 37 °C. DAPI was used as nuclear counterstaining. Slides were mounted using Prolong Gold Antifade (Thermo Fisher Scientific). Images were acquired on a Zeiss LSM 780 confocal microscope with GaAsP detector and Zen acquisition software. Images were processed using the ImageJ software and the DiD color was chosen in green.

2.5. Endosomal pH analysis

Vero cells (10^5) in 48-well plates were left untreated or treated with NH_4Cl (10 mM), bafilomycin A1 from *Streptomyces griseus* (Sigma, 1 µM final) or MGC (10 and 100 µM) for 0.5 h or 3 h, as indicated. LysoSensor Green DND-189 (Molecular Probes, 1 µM final) was added for 4 min at 37 °C before washes with PBS. Cells were detached with trypsin treatment and analyzed by flow cytometry.

2.6. Imaging flow cytometry analysis

THP-1 (10^6) cells in 0.1 ml PBS were incubated with propidium iodide (50 ng/ml) and the lipophilic probe dSQ12S (100 nM) (kind gift of Dr Klymchenko, Université de Strasbourg, France) (Collot et al., 2015) for 10 min, before addition of MGCs (100 µM) for 10 min. Amnis ImageStream^X flow cytometry analysis was performed (ImagoSeine core facility of the Institut Jacques Monod, Paris, France). Cells were imaged using Amnis ImageStream^X flow cytometry (Zuba-Surma et al., 2007) and live cells were selected as propidium iodide negative cells. The cell images were analyzed by IDEAS software (Amnis) using the Delta Centroid method to measure cell polarity (Zuba-Surma et al., 2007).

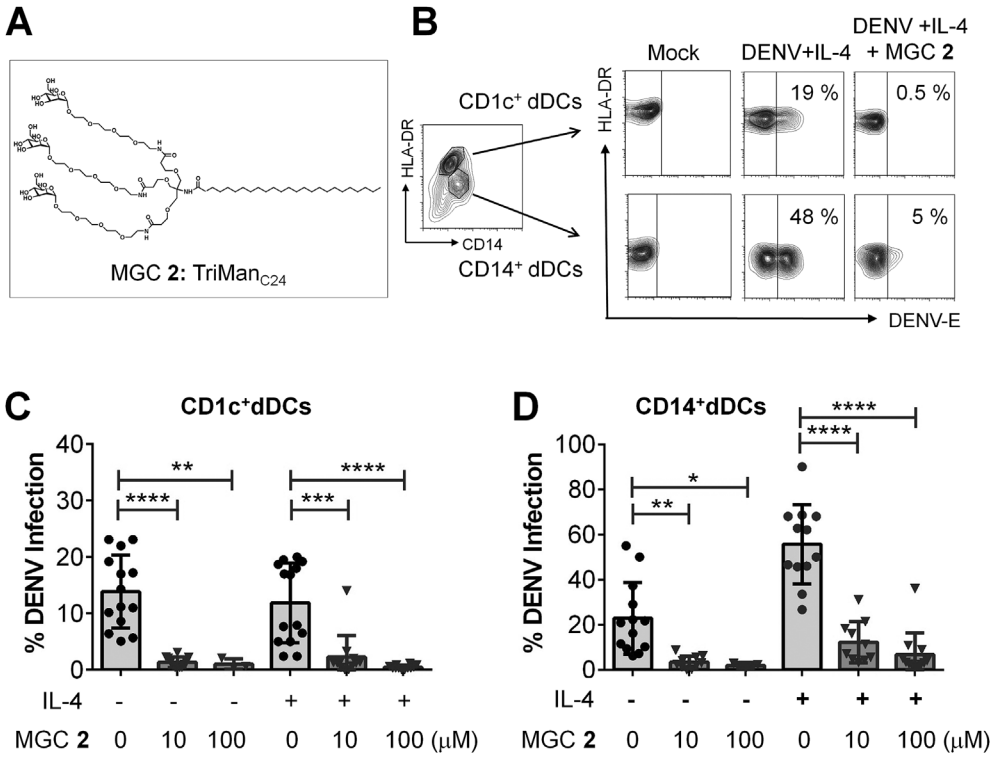

Fig. 1. Effect of MGC 2 on DENV-2 infection of human skin DCs. (A) Structure of MGC 2. (B) Representative FACS analysis of mock- or DENV-infected dermal DCs preincubated with IL-4 before addition of MGC **2** (100 μM) and the virus (MOI of 0.5). After washing and culture for 2 days, DENV infection of CD1c$^+$ dDCs (HLA-DR^{Hi}CD14$^-$) and CD14$^+$ dDCs (HLA-DR$^+$CD14$^+$) was assessed as intracellular detection of DENV-envelope (E) protein. The percentage indicates the proportion of DENV-E$^+$ cells. The graphs depict the percentage of DENV-E$^+$ CD1c$^+$dDCs (C) and DENV-E$^+$ CD14$^+$dDCs (D) as a function of MGC 2 concentrations in conditions with or without IL-4. Each symbol represents a different skin donor. Mean values (± SD) are shown as horizontal bars. (*: $p < 0.1$ **: $p < 0.01$ ***: $p < 0.001$; ****: $p < 0.0001$).

Table 1
Activities of MGC 2. IC_{50}, half maximal DENV-2 inhibitory concentration; CC_{50}, 50% cytotoxic concentration; SI, Selectivity Index, calculated as CC_{50}/IC_{50}. IC_{50} and CC_{50} values are means ± SD.

Cell type	IC_{50} (μM)	CC_{50} (μM)	SI
Dermal DCs	1.4 ± 0.7	832 ± 83	594
MDDCs	1.0 ± 0.5	1544 ± 152	1544
HepG2	4.9 ± 1.9	1165 ± 165	238

2.7. Statistical and data analysis

Graph-Pad Prism 6.01 was used for IC_{50} and CC_{50} determination by nonlinear regression, and for statistical analysis using paired Student's t-tests. Data were considered significantly different when p was less than 0.05.

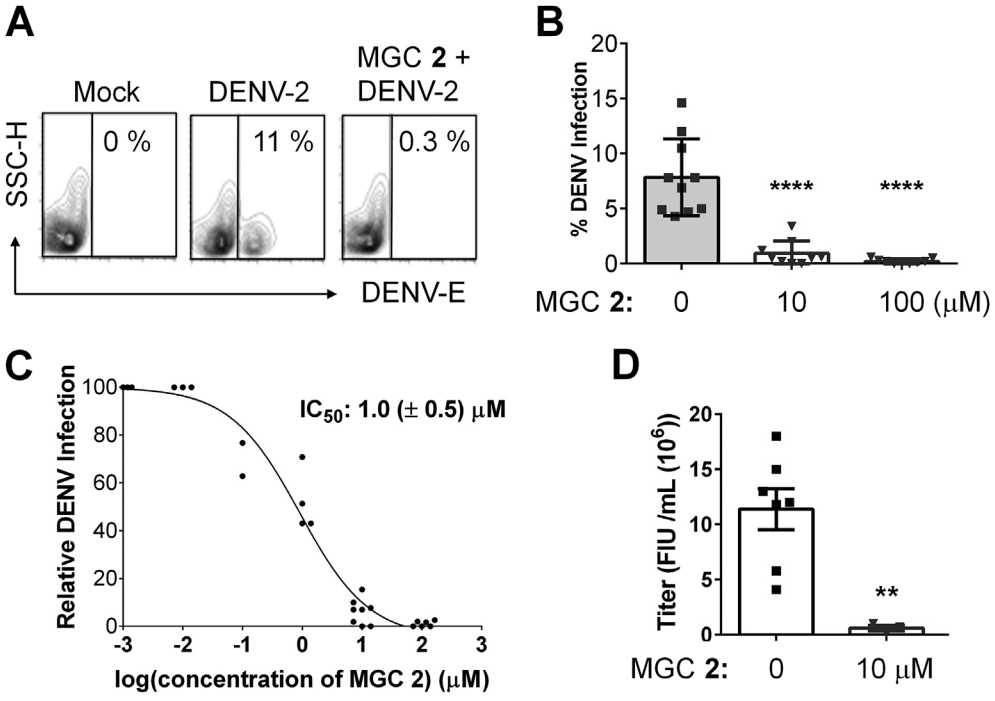

Fig. 2. MGC 2 inhibits DENV-2 infection of MDDCs. (A) Representative flow cytometry analysis of mock- or DENV-infected MDDCs preincubated with MGC 2 (100 μM) for 30 min before exposure to the virus (MOI of 0.2). The percentage of infection was measured after 2 days as the intracellular accumulation of DENV-E protein. (B) The graph depicts the percentage of infection as a function of MGC 2 concentrations. (C) Determination of the IC_{50} of MGC 2 on MDDCs. (D) Viral titers in the cell-free supernatants of DENV-infected MDDCs were determined in Vero cells as FACS infectious units (FIU/ml). For panels B–D, each symbol represents a different blood donor and the mean values (± SD) are shown as horizontal bars (****: $p < 0.0001$, **: $p < 0.01$).

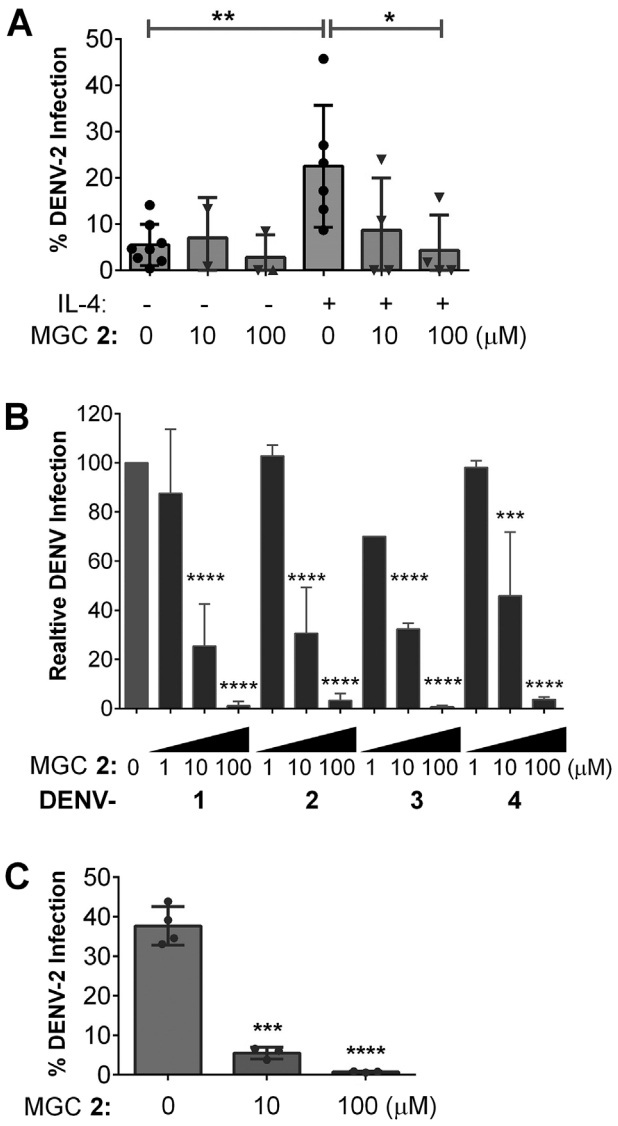

Fig. 3. Effect of MGC 2 on DENV infection of different cell types. Cells were preincubated with MGC 2 for 30 min before exposure to the virus for 2 h. The percentage of infection was measured after 2 days by FACS as the intracellular accumulation of DENV-E protein. (A) The graph depicts the percentage of dermal macrophages positive for DENV-E protein as a function of MGC concentrations for each skin donor, either untreated or IL-4-stimulated. Each donor is represented by a symbol. Mean values (± SD) are shown as horizontal bars. (B) HepG2 cells were exposed to DENV-1, -2, -3, and -4 serotypes. Histograms present the mean % of infection (± SD) relative to untreated, DENV-infected cells (at least 2 experiments in duplicate). (C) DENV-2 infection of Vero cells. Histograms present the mean values (± SD) of infection and each experiment is represented by symbol. (*: $p < 005$; **: $p < 0.01$ ***; $p < 0.001$; ****; $p < 0.0001$).

3. Results

3.1. Inhibition of DENV infection of human dermal dendritic cells

The human dermis comprises two dermal dendritic cell (DC) subsets, CD1c$^+$ and CD14$^+$, that are highly permissive to productive infection by DENV and represent an important portal to systemic spread (Cerny et al., 2014; Schaeffer et al., 2015; Schmid et al., 2014). Therefore, we investigated the anti-DENV efficacy of MGC 2 on human dermal DCs, a trimannoside linked to a 24-carbon saturated fatty acyl chain (Fig. 1A). Isolated from normal human skin, the cells were preincubated with IL-4 to increase infectivity (Schaeffer et al., 2015) and then pretreated with MGC **2** for 30 min before exposure to DENV-2. After 2 days, viral infection of the CD1c$^+$ and the CD14$^+$ DC subsets was assessed by flow cytometry by detection of intracellular DENV-2 envelope protein. 100 μM conjugate potently inhibited DENV-2 infection of both subsets (Fig. 1B). The analysis of dermal DCs from different donors in the absence or presence of IL-4 showed significant reduction of infection of both DC subsets in all conditions and with both concentrations (10 or 100 μM) (Fig. 1C and D). To determine viral progeny, we exposed Vero cells to the supernatants and determined their infection by FACS. Although not as accurate as the plaque assay (Lambeth et al., 2005), the measures showed the reduction of infectious viral particle release by MGC 2 (Supplemental Fig. S1). Toxicity measures showed minimal toxicity (CC_{50} = 921 μM ± 112) while the IC_{50} value was 1.4 μM ± 0.7 (Table 1). This shows that MGC 2 inhibits productive DENV infection of skin DCs.

3.2. Inhibition of DENV infection of human monocyte-derived DCs

Following infection of dermal DCs and macrophages, monocytes that circulate in the blood are recruited to the dermis and differentiate into monocyte-derived DCs (MDDCs). Their infection would constitute a second wave of infection in the skin (Schmid and Harris, 2014). In the light of this and because MDDCs are more easily obtained than skin DCs, we repeated the tests on MDDCs with 100 μM of MGC 2. We found that the conjugate also inhibited DENV infection of these cells (Fig. 2A). The results obtained with MDDCs derived from monocytes from different blood donors demonstrated significant inhibition of productive infection with 10 μM and 100 μM (Fig. 2B). The IC_{50} was 1.0 μM ± 0.5 (Fig. 2C) and the CC_{50} was 1544 μM ± 152 (Table 1). The infectivity of the cell supernatants titrated on Vero cells confirmed a strongly reduced production of infectious viral particles (Fig. 2D). Taken together, MGC 2 inhibits productive viral infection of *ex vivo* or monocyte-derived DCs with a high selectivity index.

3.3. MGC is active in different cell types and against different DENV serotypes

We next verified whether cell types other than DCs are sensitive to MGC inhibition. We first tested human dermal macrophages. Similar to CD14$^+$ dermal DCs, IL-4 enhanced their infection, which was inhibited by MGC 2 at 10 μM and 100 μM concentrations (Fig. 3A). Because after entry into the skin, DENV spreads systemically and can infect the liver (Martina et al., 2009), we tested hepatoma cells. The cells were infected with all four DENV serotypes, and the proportion of infected cells in the absence of MGC 2 was set to 100% for each serotype for better comparison. The results showed a dose-dependent inhibition of infection by all four serotypes (Fig. 3B), albeit with a slightly higher IC_{50} value (Table 1). Finally, given this cell-unspecific activity, we tested Vero cells. Also Vero cells were sensitive to MGC 2-mediated DENV inhibition (Fig. 3C). These findings demonstrate that MGC 2 displays a similar inhibition efficiency in unrelated cell types susceptible to DENV infection.

3.4. MGC 2 blocks DENV replication at early steps of infection

Because of its cell-indiscriminate activity, we reasoned that inhibition of infection by MGC 2 may not be mediated by cell-specific receptors. Therefore, to better understand its mode of action, we performed time-of-addition experiments in MDDCs by adding or removing the inhibitor at different time points. Results showed that 10 μM of MGC 2 abolished viral replication when present throughout (b-d) or during most (e) of the virus-cell contacts (Fig. 4A). However, infection was not reduced when MGC 2 was added to the cells and then washed off before exposure to the virus (f). This supports the notion that the conjugate does not stably interact with a viral receptor to block virus attachment. Infection also occurred when it was added after viral

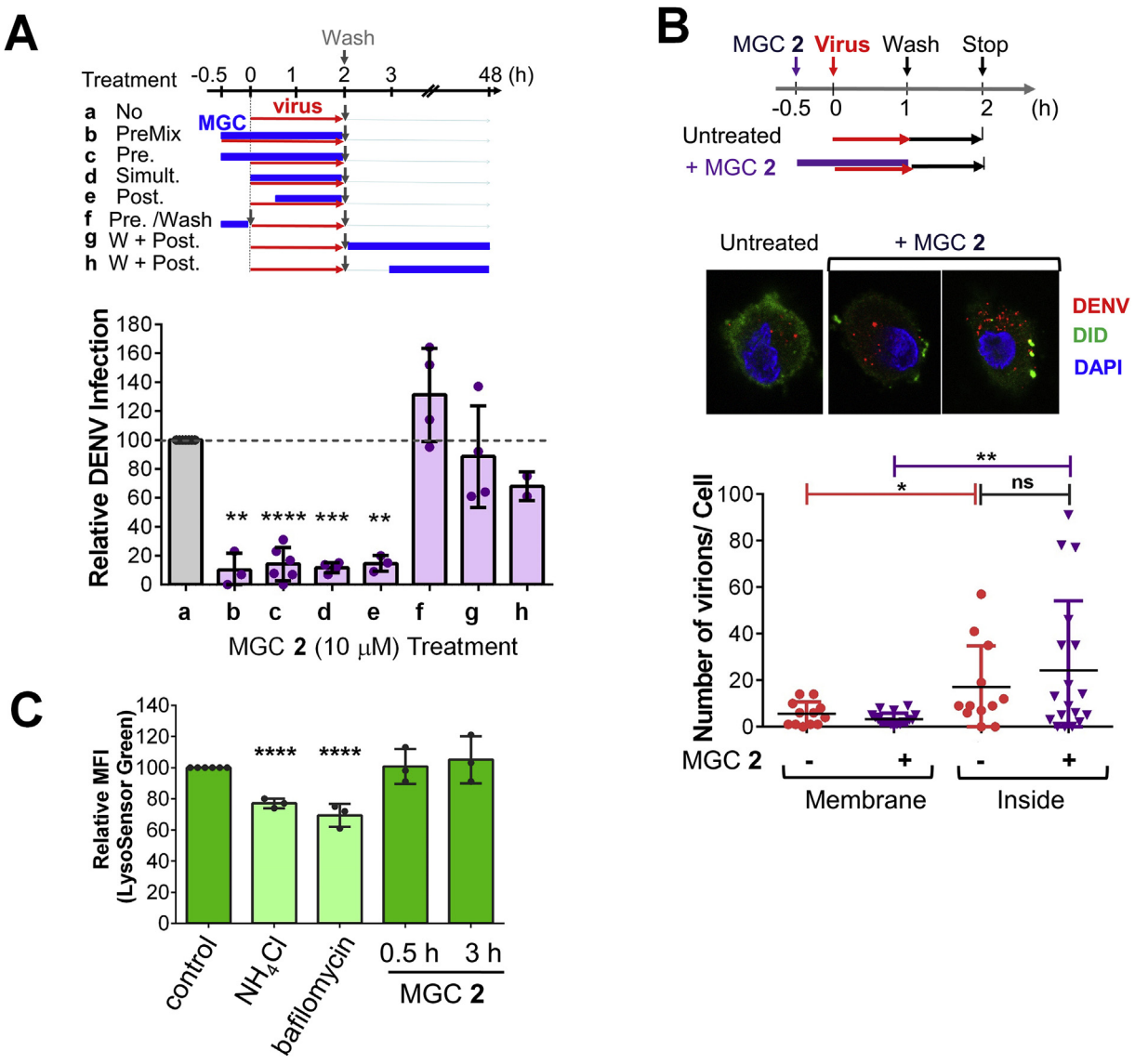

Fig. 4. MGC 2 affects early steps of the DENV replication cycle. (A) Schematic representation of time-of-addition experiments with MDDCs using MGC 2 (10 μM) and DENV-2 virus (MOI of 0.2). The graph shows the percentage of infection (± SD, 3–5 blood donors) measured after 48 h by intracellular accumulation of DENV-E protein, relative to untreated cells (condition 'a'). (B) Assessment of viral particles in MDDCs, untreated or treated with MGC 2 as indicated in the scheme. DENV, cell membrane and nucleus were identified using Cy3-conjugated mAb 4G2 (red), DiD (green) and DAPI (blue), respectively. The graph depicts the mean number of virions (± SD, 3 blood donors) on the membrane and in the cytoplasm. (C) Effect of MGC 2 on the endosomal pH. Vero cells were left untreated or treated with the inhibitors of endosomal acidification NH_4Cl and bafilomycin A1 for 3 h, or with MGC (100 μM) for 0.5 h or for 3 h. LysoSensor Green DND-189 was added for 4 min at 37 °C before flow cytometry analysis. Results show the mean fluorescence intensity (MFI, SD, 3 experiments) of LysoSensor Green relative to that of untreated cells. (**: $p < 0.01$; ***: $p < 0.001$; ****: $p < 0.0001$).

exposure and was not removed (g, h). These finding showed that the compound is active only when present during the early viral infection events.

We next sought to determine whether MGC 2 affects viral internalization. MDDCs were pretreated or not with the compound for 30 min before adding the virus (condition 'c' of Fig. 4A). After 1 h, the cells were washed free of excess virus and inhibitor, and incubated for another hour before fixing the cells for confocal microscopy (Fig. 4B). The cells were labeled with an anti-DENV-specific fluorescent antibody and with fluorescent dyes to visualize cell membrane and nucleus. As expected for a successful infection, the number of virions was higher within the cell than at the membrane; however, strikingly, this number was not significantly changed by the compound. These findings showed that MGC 2 prevented neither attachment nor internalization of DENV particles. It was notable that the distribution of the lipophilic membrane dye was different between the untreated and treated cells.

Given that the exit of the DENV RNA from endosomes into the cell cytoplasm requires low pH (Modis et al., 2004), we next asked whether endosomal pH is affected by MGC 2. Vero cells were treated with 10 μM or 100 μM of the compound or with inhibitors of endosomal acidification. After 0.5 h or 3 h, the cells were incubated with LysoSensor Green whose fluorescence is sensitive to pH (Fig. 4C and Supplemental Fig. S2). As expected, whilst NH_4Cl and bafilomycin A1 decreased the fluorescence intensity, reflecting a block in endosomal acidification, MGC 2 caused no significant change irrespective of time of exposure or concentration. Taken together, the data show that MGC 2 inhibits an event between viral uptake into endosomes and nucleic acid exit into the cytoplasm, but that does not imply an interference with endosomal acidification.

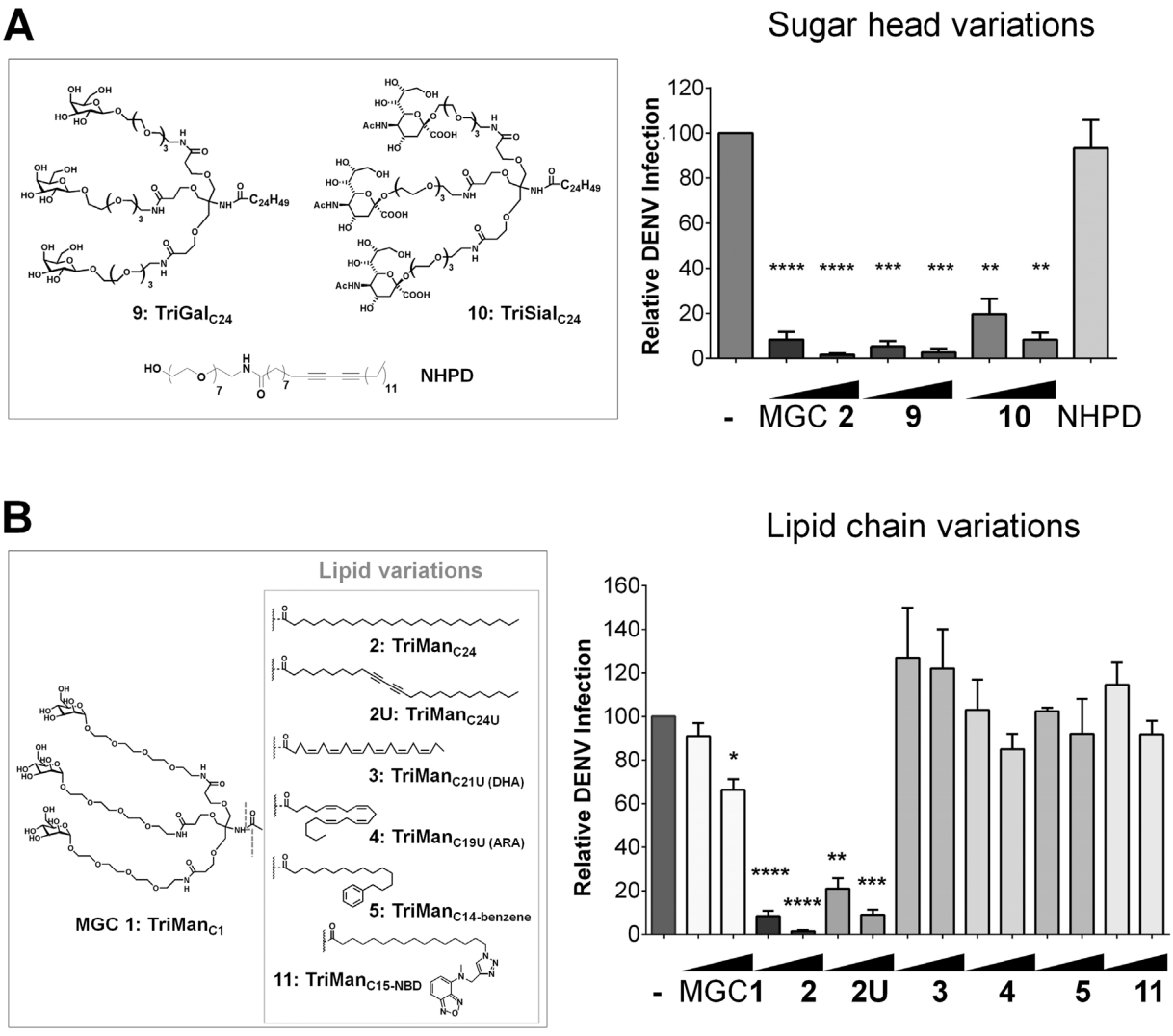

Fig. 5. Effect of sugar head and lipid chain variations of MGC 2 on DENV infection. (A) Left panel, structure of conjugates containing sugar variations (9, 10, with galactose or sialic acid) instead of mannose, or without a sugar moiety (NHPD). Right panel, MDDCs were either untreated of treated with MGC 2 or with the indicated variations of MGC 2 (concentrations of 10 and 100 μM) for 30 min before exposure to DENV-2 (MOI of 0.2). The percentage of infection was measured by intracellular accumulation of DENV-E protein and expressed as the proportion relative to the untreated control. Data are the mean ± SD of triplicates and are representative of 3 different donors. (B) Left panel, structures of conjugates containing lipid variations (1 contains no lipid chain, 2U contains an unsaturated C24 lipid chain, 3, 4 have an omega-3 and omega-6 lipid chain, conjugate 5 has a benzene-ending lipid chain, conjugate 11 contains a fluorescent NBD motif). All compounds, except 11, were previously described (Dehuyser et al., 2012; Schaeffer et al., 2013; Flacher et al., 2015). Right panel, as for panel A, only that the lipid chain was either lacking (MGC 1) or variations were introduced (MGC 2U, 3, 4, 5, 11). *: $p < 0.05$; **: $p < 0.01$; ***: $p < 0.001$ ****: $p < 0.0001$.

3.5. Structure-activity relationship studies: importance of the lipid chain

To further clarify the molecular mechanism of MGC 2 antiviral activity, improve antiviral activity and also to obtain a fluorescent derivative, we altered the sugar and lipid moieties of MGC 2. Inhibition of DENV-2 infection of MDDCs was completely lost in the absence of the sugar head (NHPD), yet replacing mannose by galactose (MGC 9) or sialic acid (MGC 10) had little impact (Fig. 5A and Supplemental Fig. S3). We designed different MGCs with variations in their lipid moiety to modulate their rigidity or flexibility (Fig. 5B). The absence of a lipid moiety (MGC 1) abolished activity. MGC 3 and 4 containing a short (19–21 carbons) polyunsaturated fatty acid chain were also inactive. Similarly, alteration of a short carbon chain with a benzene group in MGC 5 or a fluorescent NBD group in MGC 11 abolished activity. Only a minor modification introduced in the 24-carbon saturated chain of MGC 2 by replacing two saturated bonds with two unsaturations of linear geometry (MGC 2U) marginally reduced antiviral activity (Fig. 5B and Supplemental Fig. S3). These findings show that the sugar head is exchangeable, but that the lipid moiety cannot accommodate major modifications of the C24 saturated fatty acyl chain of MGC 2.

3.6. Cell membrane polarization by MGCs correlates with antiviral activity

We had previously found that MGC 2 and 2U negatively affected LPS signaling in MDDCs and altered the cell membrane distribution of the signaling receptors (Flacher et al., 2015). In addition, we have noted the effect of MGC 2 on the distribution of lipid dye DiD (Fig. 4B). Because lipid chain length and chemical composition are likely to affect the affinity of MGCs for the cell membrane, we asked whether there was a correlation between the ability to insert into the cell membrane and the antiviral activity. Since a fluorescently tagged analog of MGC 2 (MGC 11) was inactive, we addressed this question indirectly by monitoring the cell membrane distribution of the strongly fluorescent membrane dye dSQ12S (Collot et al., 2015). We compared untreated THP-1 cells with cells exposed to MGC 2, MGC 2U (slightly decreased antiviral activity) and MGC 1 (no antiviral activity). The cell

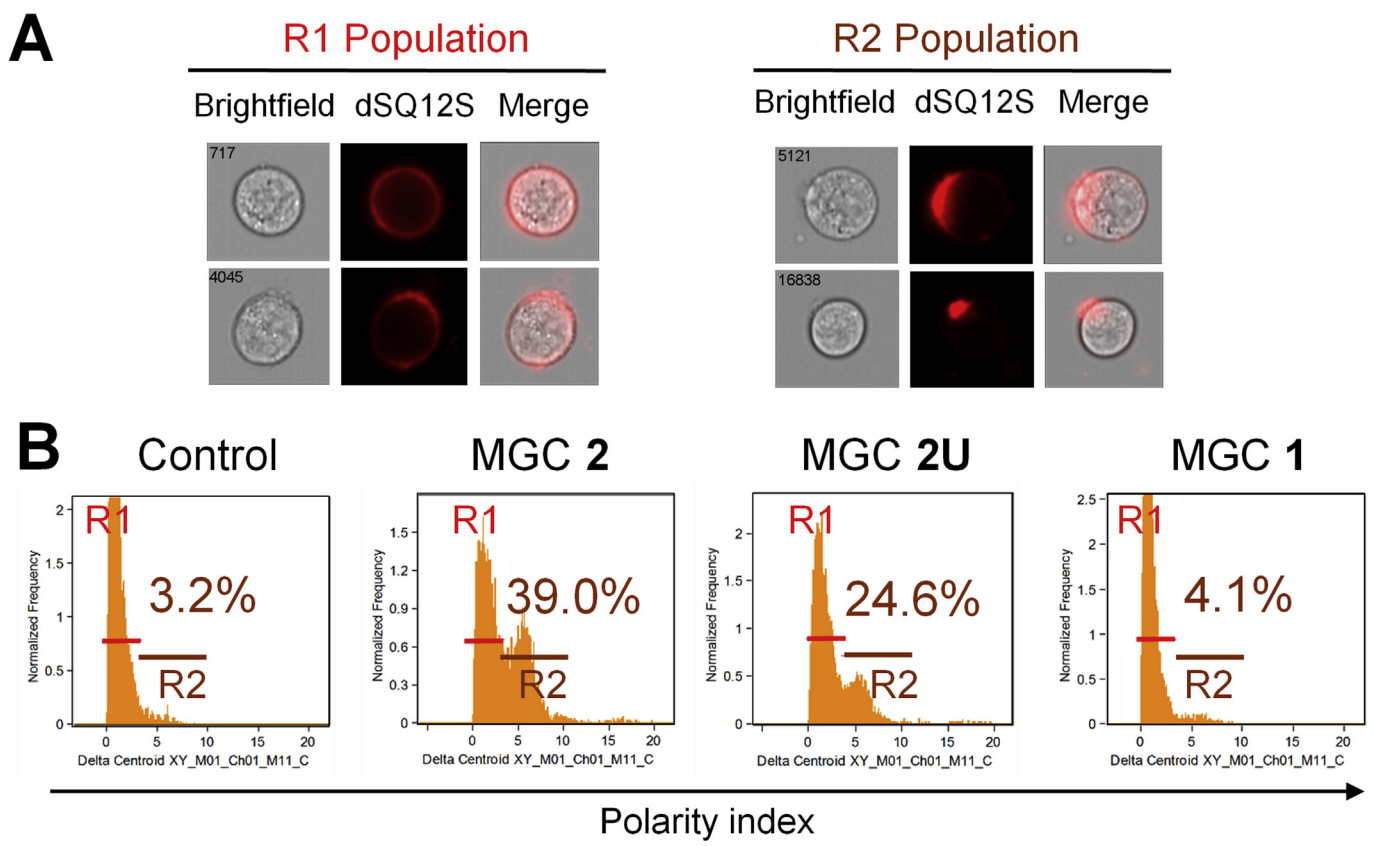

Fig. 6. MGCs affect lipid dye distribution in the plasma membrane. Amnis ImageStream^X flow cytometry analysis after incubation of THP1 cells with the lipophilic fluorescent dye dSQ12S (100 nM) for 10 min, before addition of MGCs (100 μM) for 10 min. (A) Representative images of cells of the R1 and R2 cell population. Columns on the left: brightfield; middle columns: red fluorescence of the probe, showing probe capping in R2 cells; columns on the right show brightfield merged with the fluorescence images. (B) Delta centroid cell polarity analysis showing the frequency of cells in the different conditions with uniform membrane dye staining (R1 population) and with a capped membrane distribution (R2 population). The proportion of the R2 population is indicated (representative of two experiments).

fluorescence was visualized and evaluated using imaging flow cytometry to detect slight alterations in cell membrane fluorescence patterns (Marangon et al., 2013; Zuba-Surma et al., 2007). In untreated control cells there was a homogeneous distribution of the plasma membrane dye (population R1), however 39% of the cells treated with MGC 2 displayed a polarized dye localization (population R2) (Fig. 6A and B). Strikingly, the proportion of the cells with membrane dye polarization was only 24.6% with MGC 2U and 4% with MGC 1. These findings show that the presence of the lipid and its nature disrupt the even distribution of the cell membrane dye, and the degree of disturbance correlates with the antiviral activity of the MGCs.

4. Discussion

In this study we showed that MGC 2 inhibits the productive infection of different cell types by DENV. The compound does not inhibit viral cell-entry, and the endosomes acidify normally. However, it perturbs the cell membrane, which most likely affects subsequent viral membrane-endosome fusion leading to blockage of viral genome entry into the cytoplasm.

We had previously shown that dermal CD14$^+$ DCs were highly susceptible to DENV infection that was further increased by IL-4 (Schaeffer et al., 2015). We found that even in the presence of IL-4, MGC 2 inhibited the infection of dermal DCs in the low μM range. Activity on DCs was confirmed with MDDCs. Because DCs express DC-SIGN that enhances DENV infection by binding the glycosylated viral envelope protein (Navarro-Sanchez et al., 2003; Tassaneetrithep et al., 2003), we first suspected interference of the mannosylated conjugates with DC-SIGN for binding the virus. Indeed, MGC 2 has affinity for recombinant DC-SIGN (Schaeffer et al., 2013). The lipid chain plays an important role in the affinity of MGCs to recombinant DC-SIGN (Dehuyser et al., 2012), which is most likely related to the formation of micelles and hence an increase in avidity. However, the finding that MGC 2 displays antiviral activity in hepatoma and Vero cells that lack this lectin, shows that the MGC 2 activity is not solely explained by a competition with the virus for DC-SIGN. Further, while the replacement of the mannose by a different sugar abolished interaction to DC-SIGN (Schaeffer et al., 2013), it had little impact on anti-DENV activity. On the other hand, we found that the lipid chain plays a critical role in the antiviral activity. How to consolidate these findings? All things considered, we interpret the data that MGCs in their micellar form bind with high affinity to any cell surface lectins; once bound, the micelles are disrupted to allow the lipid chain to insert into the membrane lipid bilayer. Owing to this dual function, namely formation of micelles and entry into the cell membrane, modifications of the lipid chain are poorly tolerated. In addition, the different fatty acids are likely to have an impact on cell membrane composition and physical properties. The polyunsaturated fatty acids (in MGC 3, 5) would have a favorable interaction with the non-raft membrane domains, resulting in the stabilization of the ordered rafts (Levental et al., 2016), whereas the saturated MGC 2 is likely to assemble into the ordered, saturated lipid-raft membrane domain and induces its destabilization (Sezgin et al., 2017). The more rigid MGC 2U with two triple unsaturations would be less tightly associated with the lipid raft. On this basis, MGC antiviral action would correlate with raft incorporation and destabilization.

Although our data cannot exclude a direct interaction of MGC 2

with the DENV envelope, they clearly point to a cell membrane alteration resulting in a subsequent block of virus fusion out of endosomes. Further work is required to determine in what way MGC 2 could alter the lipid/protein composition or the dynamics (stiffness versus fluidity) of the membranes.

The role of lipids in viral infection (entry, trafficking, replication and egress) is well recognized (Mazzon and Mercer, 2014); in the case of DENV, this virus utilizes a specific lipid for fusion from the late endosomes (Zaitseva et al., 2010). Thus, the pharmaceutical interference of cellular membrane composition and fluidity represents a new paradigm for broad-spectrum antiviral discovery (Pollock et al., 2010; St Vincent et al., 2010; Vigant et al., 2015). In addition to exploring the molecular interaction between MGCs and cell membrane lipids, a further question is whether MGC 2 confers protection against viruses other than DENV, given the broad-spectrum antiviral activity that results from targeting membranes. The high selectivity index of MGC 2 in human cells and its good water solubility makes this conjugate a novel and attractive candidate for further testing in cellular and animal models.

Acknowledgements

This work was supported by the “Centre National de la Recherche Scientifique” (CNRS) and the Agence Nationale de la Recherche (Program "Investissements d'Avenir" ANR-11-EQPX-022 and ANR-10-LABX-0034). We thank Sophie Reibel-Foisset (Chronobiothron, UMS 3415) for use of the L3 facilities, the IGBMC cell sorting service, the Strasbourg/Esplanade imaging platform, and Andrey Klymchenko (Strasbourg UMR 7213) for the lipid dye. We acknowledge the ImagoSeine core facility of the Institut Jacques Monod, member of IBiSA and France-BioImaging (ANR-10-INBS-04) infrastructures, and Dr Nicole Boggetto for help in the field of imaging flow cytometry.

Appendix A. Supplementary data

Supplementary data related to this article can be found at http://dx.doi.org/10.1016/j.antiviral.2018.04.005.

References

Bhatt, S., Gething, P.W., Brady, O.J., Messina, J.P., Farlow, A.W., Moyes, C.L., Drake, J.M., Brownstein, J.S., Hoen, A.G., Sankoh, O., Myers, M.F., George, D.B., Jaenisch, T., Wint, G.R., Simmons, C.P., Scott, T.W., Farrar, J.J., Hay, S.I., 2013. The global distribution and burden of dengue. Nature 496, 504–507.

Cerny, D., Haniffa, M., Shin, A., Bigliardi, P., Tan, B.K., Lee, B., Poidinger, M., Tan, E.Y., Ginhoux, F., Fink, K., 2014. Selective susceptibility of human skin antigen presenting cells to productive dengue virus infection. PLoS Pathog. 10 e1004548.

Chu, J.J., Lee, R.C., Ang, M.J., Wang, W.L., Lim, H.A., Wee, J.L., Joy, J., Hill, J., Brian Chia, C.S., 2015. Antiviral activities of 15 dengue NS2B-NS3 protease inhibitors using a human cell-based viral quantification assay. Antivir. Res. 118, 68–74.

Collot, M., Kreder, R., Tatarets, A.L., Patsenker, L.D., Mely, Y., Klymchenko, A.S., 2015. Bright fluorogenic squaraines with tuned cell entry for selective imaging of plasma membrane vs. endoplasmic reticulum. Chem. Commun. 51, 17136–17139.

Dehuyser, L., Schaeffer, E., Chaloin, O., Mueller, C.G., Baati, R., Wagner, A., 2012. Synthesis of novel mannoside glycolipid conjugates for inhibition of HIV-1 trans-infection. Bioconjugate Chem. 23, 1731–1739.

Diamond, M.S., Zachariah, M., Harris, E., 2002. Mycophenolic acid inhibits Dengue virus infection by preventing replication of viral RNA. Virology 304, 211–221.

Duyen, H.T.L., Cerny, D., Trung, D.T., Pang, J., Velumani, S., Toh, Y.X., Qui, P.T., Hao, N.V., Simmons, C., Haniffa, M., Wills, B., Fink, K., 2017. Skin dendritic cell and T cell activation associated with dengue shock syndrome. Sci. Rep. 7, 14224.

Flacher, V., Neuberg, P., Point, F., Daubeuf, F., Muller, Q., Sigwalt, D., Fauny, J.D., Remy, J.S., Frossard, N., Wagner, A., Mueller, C.G., Schaeffer, E., 2015. Mannoside glycolipid conjugates display anti-inflammatory activity by inhibition of Toll-like receptor-4 mediated cell activation. ACS Chem. Biol. 10, 2697–2705.

Hyrina, A., Meng, F., McArthur, S.J., Eivemark, S., Nabi, I.R., Jean, F., 2017. Human Subtilisin Kexin Isozyme-1 (SKI-1)/Site-1 Protease (S1P) regulates cytoplasmic lipid droplet abundance: a potential target for indirect-acting anti-dengue virus agents. PLoS One 12 e0174483.

Ivory, M.O., Birchall, J.C., Piguet, V., 2015. Early dengue virus infection in human skin: a cycle of inflammation and infectivity. J. Invest. Dermatol. 135, 1711–1712.

Jadav, S.S., Kaptein, S., Timiri, A., De Burghgraeve, T., Badavath, V.N., Ganesan, R., Sinha, B.N., Neyts, J., Leyssen, P., Jayaprakash, V., 2015. Design, synthesis, optimization and antiviral activity of a class of hybrid dengue virus E protein inhibitors. Bioorg. Med. Chem. Lett. 25, 1747–1752.

Julander, J.G., Perry, S.T., Shresta, S., 2011. Important advances in the field of anti-dengue virus research. Antivir. Chem. Chemother. 21, 105–116.

Kaptein, S.J., Neyts, J., 2016. Towards antiviral therapies for treating dengue virus infections. Curr. Opin. Pharmacol. 30, 1–7.

Kaufmann, B., Rossmann, M.G., 2011. Molecular mechanisms involved in the early steps of flavivirus cell entry. Microbes Infect. 13, 1–9.

Lambeth, C.R., White, L.J., Johnston, R.E., de Silva, A.M., 2005. Flow cytometry-based assay for titrating dengue virus. J. Clin. Microbiol. 43, 3267–3272.

Levental, K.R., Lorent, J.H., Lin, X., Skinkle, A.D., Surma, M.A., Stockenbojer, E.A., Gorfe, A.A., Levental, I., 2016. Polyunsaturated lipids regulate membrane domain stability by tuning membrane order. Biophys. J. 110, 1800–1810.

Lo, Y.C., Perng, G.C., 2016. Novel concept on antiviral strategies to dengue. Curr. Opin. Virol. 18, 97–108.

Marangon, I., Boggetto, N., Menard-Moyon, C., Luciani, N., Wilhelm, C., Bianco, A., Gazeau, F., 2013. Localization and relative quantification of carbon nanotubes in cells with multispectral imaging flow cytometry. J. Vis. Exp. e50566.

Martina, B.E., Koraka, P., Osterhaus, A.D., 2009. Dengue virus pathogenesis: an integrated view. Clin. Microbiol. Rev. 22, 564–581.

Mazzon, M., Mercer, J., 2014. Lipid interactions during virus entry and infection. Cell. Microbiol. 16, 1493–1502.

Miller, J.L., de Wet, B.J., Martinez-Pomares, L., Radcliffe, C.M., Dwek, R.A., Rudd, P.M., Gordon, S., 2008. The mannose receptor mediates dengue virus infection of macrophages. PLoS Pathog. 4, e17.

Modis, Y., Ogata, S., Clements, D., Harrison, S.C., 2004. Structure of the dengue virus envelope protein after membrane fusion. Nature 427, 313–319.

Navarro-Sanchez, E., Altmeyer, R., Amara, A., Schwartz, O., Fieschi, F., Virelizier, J.L., Arenzana-Seisdedos, F., Despres, P., 2003. Dendritic-cell-specific ICAM3-grabbing non-integrin is essential for the productive infection of human dendritic cells by mosquito-cell-derived dengue viruses. EMBO Rep. 4, 723–728.

Noble, C.G., Chen, Y.L., Dong, H., Gu, F., Lim, S.P., Schul, W., Wang, Q.Y., Shi, P.Y., 2010. Strategies for development of Dengue virus inhibitors. Antivir. Res. 85, 450–462.

Pollock, S., Nichita, N.B., Bohmer, A., Radulescu, C., Dwek, R.A., Zitzmann, N., 2010. Polyunsaturated liposomes are antiviral against hepatitis B and C viruses and HIV by decreasing cholesterol levels in infected cells. Proc. Natl. Acad. Sci. U. S. A. 107, 17176–17181.

Rather, I.A., Parray, H.A., Lone, J.B., Paek, W.K., Lim, J., Bajpai, V.K., Park, Y.H., 2017. Prevention and control strategies to counter dengue virus infection. Front. Cell. Infect. Microbiol. 7, 1–8.

Schaeffer, E., Dehuyser, L., Sigwalt, D., Flacher, V., Bernacchi, S., Chaloin, O., Remy, J.S., Mueller, C.G., Baati, R., Wagner, A., 2013. Dynamic micelles of mannoside glycolipids are more efficient than polymers for inhibiting HIV-1 trans-infection. Bioconjugate Chem. 24, 1813–1823.

Schaeffer, E., Flacher, V., Papageorgiou, V., Decossas, M., Fauny, J.D., Kramer, M., Mueller, C.G., 2015. Dermal CD14(+) dendritic cell and macrophage infection by dengue virus is stimulated by Interleukin-4. J. Invest. Dermatol. 135, 1743–1751.

Schmid, M.A., Diamond, M.S., Harris, E., 2014. Dendritic cells in dengue virus infection: targets of virus replication and mediators of immunity. Front. Immunol. 5, 1–10.

Schmid, M.A., Harris, E., 2014. Monocyte recruitment to the dermis and differentiation to dendritic cells increases the targets for dengue virus replication. PLoS Pathog. 10, e1004541.

Sezgin, E., Levental, I., Mayor, S., Eggeling, C., 2017. The mystery of membrane organization: composition, regulation and roles of lipid rafts. Nat. Rev. Mol. Cell. Biol. 18, 361–374.

St Vincent, M.R., Colpitts, C.C., Ustinov, A.V., Muqadas, M., Joyce, M.A., Barsby, N.L., Epand, R.F., Epand, R.M., Khramyshev, S.A., Valueva, O.A., Korshun, V.A., Tyrrell, D.L., Schang, L.M., 2010. Rigid amphipathic fusion inhibitors, small molecule antiviral compounds against enveloped viruses. Proc. Natl. Acad. Sci. U. S. A. 107, 17339–17344.

Stanaway, J.D., Shepard, D.S., Undurraga, E.A., Halasa, Y.A., Coffeng, L.E., Brady, O.J., Hay, S.I., Bedi, N., Bensenor, I.M., Castaneda-Orjuela, C.A., Chuang, T.W., Gibney, K.B., Memish, Z.A., Rafay, A., Ukwaja, K.N., Yonemoto, N., Murray, C.J.L., 2016. The global burden of dengue: an analysis from the Global Burden of Disease Study 2013. Lancet Infect. Dis. 16, 712–723.

Tassaneetrithep, B., Burgess, T.H., Granelli-Piperno, A., Trumpfheller, C., Finke, J., Sun, W., Eller, M.A., Pattanapanyasat, K., Sarasombath, S., Birx, D.L., Steinman, R.M., Schlesinger, S., Marovich, M.A., 2003. DC-SIGN (CD209) mediates dengue virus infection of human dendritic cells. J. Exp. Med. 197, 823–829.

Vigant, F., Santos, N.C., Lee, B., 2015. Broad-spectrum antivirals against viral fusion. Nat. Rev. Microbiol. 13, 426–437.

Zaitseva, E., Yang, S.T., Melikov, K., Pourmal, S., Chernomordik, L.V., 2010. Dengue virus ensures its fusion in late endosomes using compartment-specific lipids. PLoS Pathog. 6 e1001131.

Zuba-Surma, E.K., Kucia, M., Abdel-Latif, A., Lillard Jr., J.W., Ratajczak, M.Z., 2007. The ImageStream System: a key step to a new era in imaging. Folia histochem. Cytobiol. 45, 279–290.